Overexpression of decorin gene influences the biological behaviors of follicular thyroid carcinoma cells

QIANHUANG LIN, YE MA, RUNSHENG GUO, HAILONG GUO, XIAOYUN WANG and TING YANG

Department of General Surgery, Jiading District Central Hospital Affiliated Shanghai University of Medicine and Health Sciences, Shanghai 201800, P.R. China

Received January 30, 2025; Accepted April 29, 2025

DOI: 10.3892/ol.2025.15120

Abstract. The objective of the present study was to examine the impact of decorin (DCN) gene overexpression on the proliferation, migration and invasion of human follicular thyroid carcinoma (FTC) cells. DCN expression was evaluated by western blotting (WB) in Nthy-ori3-1 normal thyroid cells and in two FTC cell lines, namely FTC-133 and FTC-238. Lentiviral transfection was employed to overexpress DCN in the FTC cells, with the overexpression efficiency confirmed through reverse transcription-quantitative polymerase chain reaction and WB. Cell viability, colony formation, wound healing and Transwell invasion assays were conducted to assess the proliferation, migration and invasion of the transfected cells. The results revealed that DCN expression in FTC-133 and FTC-238 cells was significantly lower compared with that in Nthy-ori3-1 cells. Successful lentiviral overexpression of DCN in the FTC cell lines significantly decreased the proliferation and colony formation abilities of the cells, and diminished their wound healing and invasive capabilities. This indicated that the lentivirus-mediated overexpression of DCN in FTC-133 and FTC-238 cells altered their cellular behavior, providing experimental evidence to support the suggestion that DCN is a potential therapeutic target for FTC.

Introduction

In recent decades, there has been a notable increase in the global incidence of differentiated thyroid cancer (DTC). According to GLOBOCAN 2020 data on cancer incidence and mortality, thyroid cancer ranks ninth overall and fifth among female malignancies for incidence (1). Follicular thyroid carcinoma (FTC) is a relatively uncommon subtype of DTC that originates from thyroid follicular cells. Its incidence is markedly lower than that of papillary thyroid carcinoma (PTC), accounting for 5-15% of all thyroid malignancies. However, FTC exhibits higher malignancy compared with PTC, demonstrating a tendency for hematogenous spread and a higher risk of distant metastasis. The most frequent sites of FTC metastasis are the bones and lungs (2-4). The prognosis of FTC primarily depends on the clinical stage at diagnosis, with early diagnosis and treatment generally associated with more favorable outcomes. By contrast, advanced or recurrent cases tend to have a less favorable prognosis. In addition, FTC is more susceptible to dedifferentiation and resistance to radioactive iodine (RAI) therapy (5), which complicates clinical management by limiting therapeutic options and increasing the risk of disease progression and recurrence.

Decorin (DCN) is a small leucine-rich proteoglycan (PG) predominantly present in the extracellular matrix of mammalian connective tissues. This protein exhibits diverse biological functions, including inhibition of collagen fiber formation and regulation of cell proliferation, migration and adhesion (6). While the role of DCN in breast, liver and colorectal cancers is well documented (7-12), its involvement in FTC remains poorly characterized. An early study by Arnaldi *et al* (13) demonstrated the downregulation of DCN mRNA levels in FTC tissues, a finding later corroborated at the protein level by our previous study in which FTC and adjacent noncancerous tissues were compared (14). However, the functional relevance of DCN downregulation to the pathogenesis of FTC, particularly its impact on tumor cell behavior, has not yet been elucidated. Therefore, the present study sought to clarify the role of DCN in the progression of FTC. By comprehensively examining the association between DCN expression levels and the proliferation, migration and invasion capabilities of FTC cells, the study aimed to provide evidence supporting the potential of DCN as a therapeutic target for this malignancy.

Materials and methods

Main materials. The Nthy-ori3-1 human noncancerous thyroid cell line and FTC-133 human FTC cell line were acquired from iCell Bioscience Inc. Another human FTC cell line, FTC-238, was obtained from Shanghai WheLab Bioscience Ltd. Dulbecco's Modified Eagle's Medium (DMEM)/F12 and RPMI-1640 cell

Correspondence to: Professor Ting Yang, Department of General Surgery, Jiading District Central Hospital Affiliated Shanghai University of Medicine and Health Sciences, 1 Chengbei Road, Jiading, Shanghai 201800, P.R. China
E-mail: dr_yangting@163.com

Key words: follicular thyroid carcinoma, decorin, lentivirus, gene overexpression, biological behavior

culture media were sourced from iCell Bioscience Inc., while Gibco fetal bovine serum (FBS) was purchased from Thermo Fisher Scientific, Inc. Penicillin-streptomycin and trypsin solutions were obtained from Beyotime Institute of Biotechnology. The bicinchoninic acid (BCA) protein quantitative kit was also procured from Beyotime Institute of Biotechnology. Primary antibodies against DCN and β-actin, as well as Cell Counting Kit-8 (CCK-8) reagents, were acquired from Wuhan Sanying Biotechnology. The Transwell chamber was obtained from Corning, Inc. The quantitative polymerase chain reaction (qPCR) kit and total RNA extraction kit (Vazyme FastPure Cell/Tissue Total RNA Isolation Kit V2; cat. no. RC112-01) were sourced from Vazyme Biotech Co., Ltd., while the reverse transcription (RT) kit was procured from Takara Bio, Inc. Lentiviruses (pcSLenti-EF1-EGFP-P2A-Puro-CMV-DCN-3xFLAG-WPRE; 3rd generation lentiviral system) for the overexpression of DCN and for use as a transfection control were designed and packaged by OBiO Technology (Shanghai) Corp., Ltd.

Cell culture. Nthy-ori3-1 and FTC-133 cells were maintained in RPMI-1640 and the FTC-238 cells were cultured in DMEM/F12; both media were supplemented with 1% penicillin-streptomycin solution and 10% FBS. All cells were incubated at 37˚C with 5% CO_2, with the cell culture medium refreshed every 24-48 h based on cell confluency. Upon reaching 90% confluency, adherent cells were detached using trypsin solution and passaged for subsequent experiments up to the sixth or seventh generation. All cell culture procedures were conducted under sterile conditions, and all experiments utilized cells in the logarithmic growth phase.

RT-qPCR. Total RNA was extracted from cells in each group during the logarithmic growth phase using a Vazyme FastPure Kit (cat. no. RC112-01). An ultra-microspectrophotometer was utilized to determine the total RNA concentration of the extract. Following this, cDNA synthesis was performed using the Takara PrimeScript™ RT reagent Kit with gDNA Eraser (Perfect Real Time; cat. no. RR047A). Briefly, genomic DNA was removed by incubation at 42˚C for 2 min, and reverse transcription was conducted at 37˚C for 15 min using the kit's RT Primer Mix. The reaction was terminated by heating at 85˚C for 5 sec to inactivate the enzyme, as per the manufacturer's guidelines. Then, qPCR was carried out using a SYBR Green-based master mix on the Analytik Jena qTOWER3 Real-Time PCR System (Model: qTOWER3G; Analytik Jena GmbH). The thermal cycling protocol included an initial denaturation step at 95˚C for 3 min, followed by 40 cycles of amplification consisting of denaturation at 95˚C for 5 sec and a combined annealing/extension step at 60˚C for 5 sec, with fluorescence signal acquisition at the end of the annealing/extension phase. To validate amplification specificity, a melting curve analysis was subsequently performed by gradually heating the samples from 65 to 95˚C at a rate of 0.5˚C per increment. All reactions were conducted in triplicate to ensure technical reproducibility. DCN RNA expression levels were normalized to those of the internal reference β-actin, and the relative mRNA expression level of DCN was calculated using the $2^{-\Delta\Delta Cq}$ method (15). Table I lists the sequences of the primers used.

Western blotting (WB). The cells in each group were lysed on ice using RIPA lysis buffer [50 mM Tris (VETEC), 150 mM NaCl [Tianjin DaMao Chemical Reagent Partnership (Limited Partnership)], 1% Triton X-100 (Jianglai Bio; Shanghai Future Industrial Co., Ltd.), 0.1% SDS (Vetec), 1% sodium deoxycholate (Zeye Biological), 1 mM EDTA (Amresco, LLC), supplemented with 5 mM NaF (Shanghai Macklin Biochemical Co., Ltd.), 2 mM sodium pyrophosphate (Shanghai Qincheng Biotechnology Co., Ltd.), 2 mM β-glycerophosphate (Qimin Bio, www.shkambio.com), 1 mM Na3VO4 (Shanghai Baishun Biotechnology Co., Ltd.), 1 mM PMSF (Beyotime Institute of Biotechnology) and protease inhibitor cocktail (Beijing Biolab Technology Co., Ltd.); all stored at 4˚C protected from light]. The protein concentration of the lysate was determined using a BCA protein assay kit. Then, equal amounts of proteins (20 μg per lane) were separated via 10% sodium dodecyl sulfate-polyacrylamide gel electrophoresis, transferred to a PVDF membrane, and blocked with 1X Tris-buffered saline with 0.1% Tween-20 (TBST) containing 5% skimmed milk for 1 h at 25˚C. The membranes were then incubated with primary antibodies against DCN (cat. no. 14667; 1:1,000; Proteintech Group, Inc.) and β-actin (cat. no. 66009-1-Ig; 1:5,000; Proteintech Group, Inc.) at room temperature (25˚C) for 1 h. After washing five times with 1X TBST, HRP-conjugated goat anti-rabbit secondary antibodies (cat. no. GNI9310-R) diluted 1:5,000 in blocking buffer were added, and the membranes were incubated at room temperature for an additional 1 h. Following five more washes with 1X TBST, the target protein bands were visualized utilizing an enhanced chemiluminescence reagent (Ultrasensitive ECL; cat. no. 1810202; Shanghai Qinxiang Scientific Instrument Co., Ltd.), with the images generated and captured by a gel imaging system. Protein band intensities were analyzed using ImageJ software (version 1.54g; National Institutes of Health), supported by Java 1.8.0_345 (64-bit). Finally, the relative expression of DCN was evaluated, using β-actin as an internal reference.

Lentiviral infection. FTC-133 and FTC-238 cells were divided into a negative control (NC) group and a DCN overexpression (OE-DCN) group, which were respectively infected with control lentiviral particles and recombinant lentiviral particles carrying the DCN gene. Lentiviral infection was performed using optimized multiplicities of infection of 80 for FTC-133 cells and 10 for FTC-238 cells. Recombinant lentiviral particles carrying the DCN gene [titer, $2.41x10^9$ transducing units (TU)/ml] and control particles (titer, $1.69x10^9$ TU/ml) were used. After 12 h, the medium was replaced with fresh complete medium. Stably transduced cells were selected using 1 μg/ml puromycin for 7-14 days until all uninfected cells were eliminated. Overexpression efficiency was validated by fluorescence microscopy [≥80% green fluorescent protein $(GFP)^+$ cells], RT-qPCR and WB.

Cell viability assay. Transfected FTC-133 and FTC-238 cells (OE-DCN and NC groups for each cell line) in the logarithmic growth phase were seeded into 96-well plates at a density of 3,000 cells/well. Following incubation for 0, 24, 48, 72 and 96 h, CCK-8 reagent (10 μl/well) was added and the cells were incubated at 37˚C for 1-4 h to ensure measurements within the linear detection range (optimized via preliminary tests).

Table I. Primer sequences utilized for quantitative polymerase chain reaction.

ID	Sequence (5'- 3')
β-actin-F	CCTGGCACCCAGCACAAT
β-actin-R	GGGCCGGACTCGTCATAC
DCN-F	GGCTGGACCGTTTCAACAGAGAG
DCN-R	AAGATGGCATTGACAGCGGAAGG

DCN, decorin; F, forward; R, reverse.

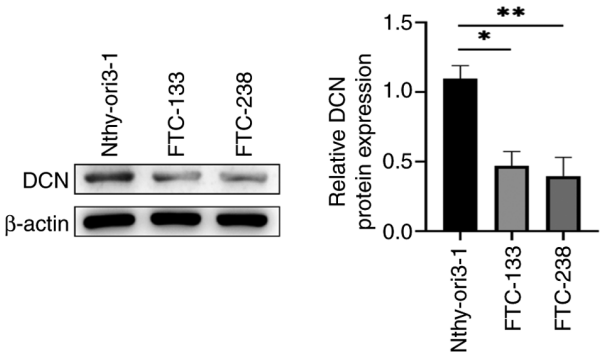

Figure 1. DCN expression in follicular thyroid carcinoma and noncancerous thyroid cell lines. Representative western blots and quantified results are presented. *P<0.05 and **P<0.01 as indicated. DCN, decorin.

The optical density at 450 nm was measured at multiple time points (1, 2, 3 and 4 h) using a microplate reader, and the 2-h time point (within the linear phase, R^2>0.98) was selected for final analysis. Cell growth curves were then generated based on these measurements.

Colony formation assays. Transfected FTC 133 and FTC-238 cells were trypsinized, counted and seeded into 6-well plates at a density of 700 cells/well. The cells were incubated at 37˚C for 14 days. If any colony reached ≥50 cells prior to the 14-day endpoint, the culture was immediately terminated and analyzed; otherwise, incubation proceeded for the full duration. Afterwards, the cells were gently washed once with PBS and fixed with 1 ml 4% paraformaldehyde for 45 min at 25˚C. Following fixation, the wells were washed with PBS and stained with 1 ml/well crystal violet dye for 20 min at 25˚C. Finally, the cells were thoroughly rinsed with PBS and allowed to air-dry. Images were captured against a white background, and colonies (defined as cell clusters containing ≥50 adherent cells) were quantified using ImageJ software. Cell counts were performed on the same images to assess viability.

Transwell assay. The invasive ability of the FTC cells was assessed by Transwell assays, conducted using Matrigel-coated chambers (pre-coated with 80 μl of BD Matrigel diluted 1:8 in serum-free medium, followed by polymerization at 37˚C for 30 min) in 12-well plates. The upper and lower chambers were first washed once with 200 and 500 μl serum-free medium, respectively. Cell suspensions ($5x10^4$ cells/ml) from each experimental group were prepared using serum-free medium. A 200-μl aliquot of cell suspension was introduced into the upper chamber, while the lower chamber was filled with 500 μl complete medium supplemented with 20% FBS. Following a 48-h incubation period at 37˚C, the chambers were removed and washed with PBS to eliminate residual media. The cells were then stained with crystal violet solution for 20 min at room temperature (25˚C). Excess stain was removed with distilled water, and cells on the upper surface of the membrane were carefully removed using a cotton swab. Cells that had invaded through the membrane were visualized and photographed using a widefield inverted fluorescence microscope (Model: MC-D500U3; Jiangxi Phoenix Optics Group Co., Ltd.). Three randomly selected fields from each well were analyzed to count the number of invading cells.

Wound healing assay. The transfected FTC-133 and FTC-238 cells were seeded into a 6-well plate with a total of $5x10^5$ cells/well and cultured with 2 ml complete medium containing 10% FBS (Gibco; Thermo Fisher Scientific, Inc.; cat. no. 10270-106) in a 5% CO_2 incubator at 37˚C. When the cell confluency reached 80-90%, a scratch wound was created in the cells using a 200-μl pipette tip. Immediately after scratching, the medium was replaced with serum-free medium to minimize the effect on proliferation. The wound was photographed using an inverted light microscope (MC-D500U3; Jiangxi Phoenix Optics Group Co., Ltd.) at x4 magnification, and its width was recorded as the initial wound size. The 6-well plate was then returned to the 37˚C, 5% CO_2 incubator. After 6, 12, 24, 48 and 72 h of incubation, the wound width was measured at the same location. Cell motility was calculated using the formula: Cell motility (%)=[(initial scratch width - scratch width after migration)/initial scratch width] x100. The experiments were performed in triplicate, and the results were averaged for statistical analysis.

Statistical analysis. Statistical analysis and the visualization of experimental data were performed using GraphPad Prism 8.0 software (Dotmatics). Measurement data are presented as the mean ± standard deviation. For comparisons between two groups, unpaired Student's t-test was employed. For comparisons among multiple groups, one-way analysis of variance followed by Tukey's post hoc test was used to assess pairwise differences. P<0.05 was considered to indicate a statistically significant difference.

Results

FTC cells express low levels of DCN. The expression levels of DCN in FTC and noncancerous thyroid cell lines were compared. WB revealed that the expression levels of DCN in the FTC cell lines were significantly lower compared with those in the Nthy-ori3-1 noncancerous thyroid cell line (P<0.05; Fig. 1).

Establishment of DCN-overexpressing FTC cell lines. To investigate the impact of DCN overexpression on FTC cells, FTC-133 and FTC-238 cell lines were infected with lentiviral particles overexpressing both DCN and enhanced green fluorescent

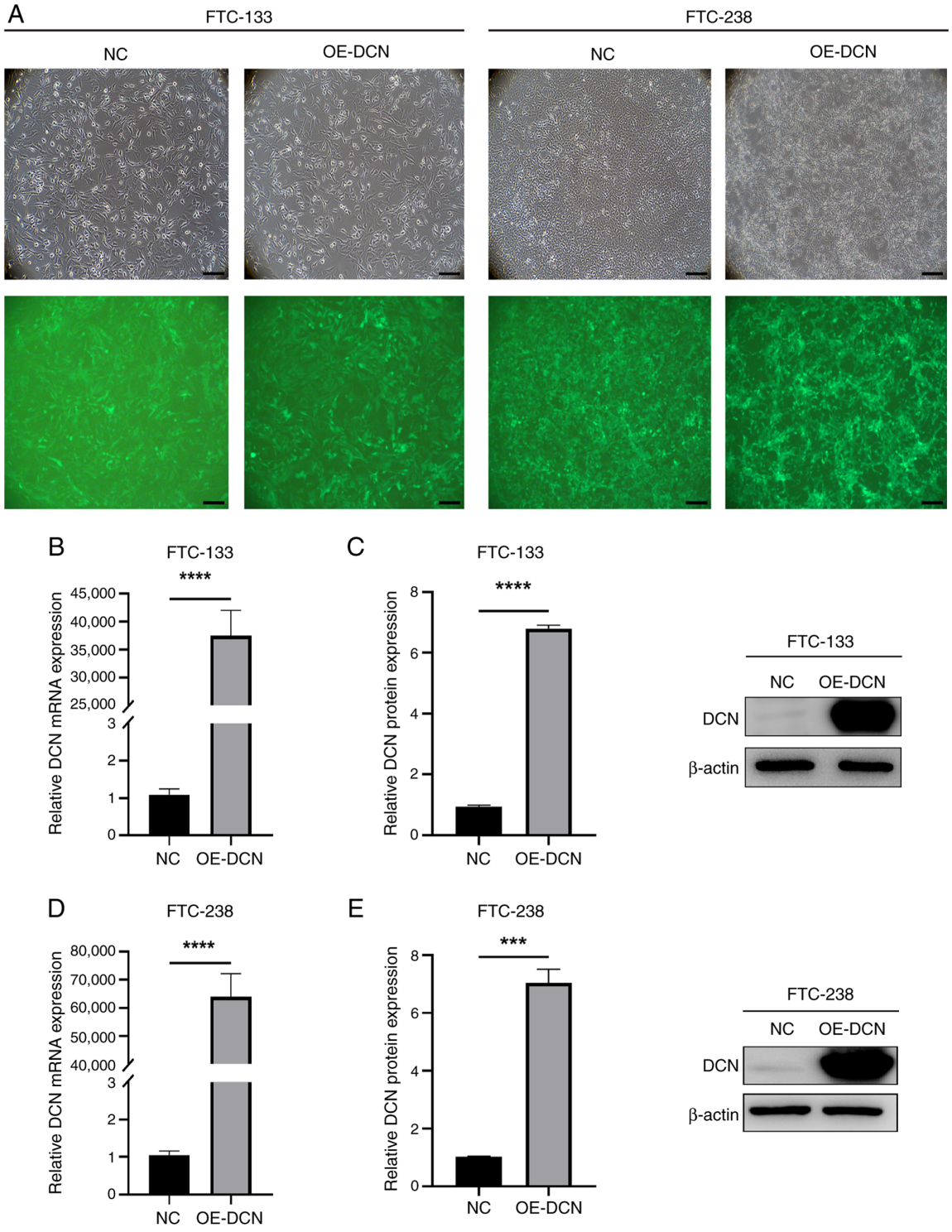

Figure 2. Successful establishment of DCN-overexpressing FTC-133 and FTC-238 cells. (A) Microscopy images of FTC-133 and FTC-238 cells, including fluorescence images showing EGFP expression. The EGFP marker indicates successful lentiviral infection. Scale bar, 100 μm. (B) mRNA and (C) protein levels of DCN in FTC-133 cells infected with DCN-overexpressing lentivirus. (D) mRNA and (E) protein levels of DCN in FTC-238 cells infected with DCN-overexpressing lentivirus. ***P<0.001 and ****P<0.0001 as indicated. DCN, decorin; OE-DCN, DCN overexpression group; NC, negative control group.

protein as a reporter gene to establish two cellular models of DCN overexpression. As shown by the fluorescence microscopy images in Fig. 2A, the infection rates for the FTC-133 and FTC-238 cell lines were ≥90%. In addition, RT-qPCR analyses revealed that DCN mRNA expression levels in the OE-DCN groups were significantly increased compared with those in the corresponding NC groups (P<0.0001; Fig. 2B and D). WB analyses corroborated the RT-qPCR results, with significantly increased DCN protein expression levels in the OE-DCN groups compared with those in the corresponding NC groups (P<0.001; Fig. 2C and E).

DCN overexpression suppresses the proliferation of FTC cells. The effect of DCN overexpression on the proliferation of FTC cells was investigated. In the colony formation assay, the

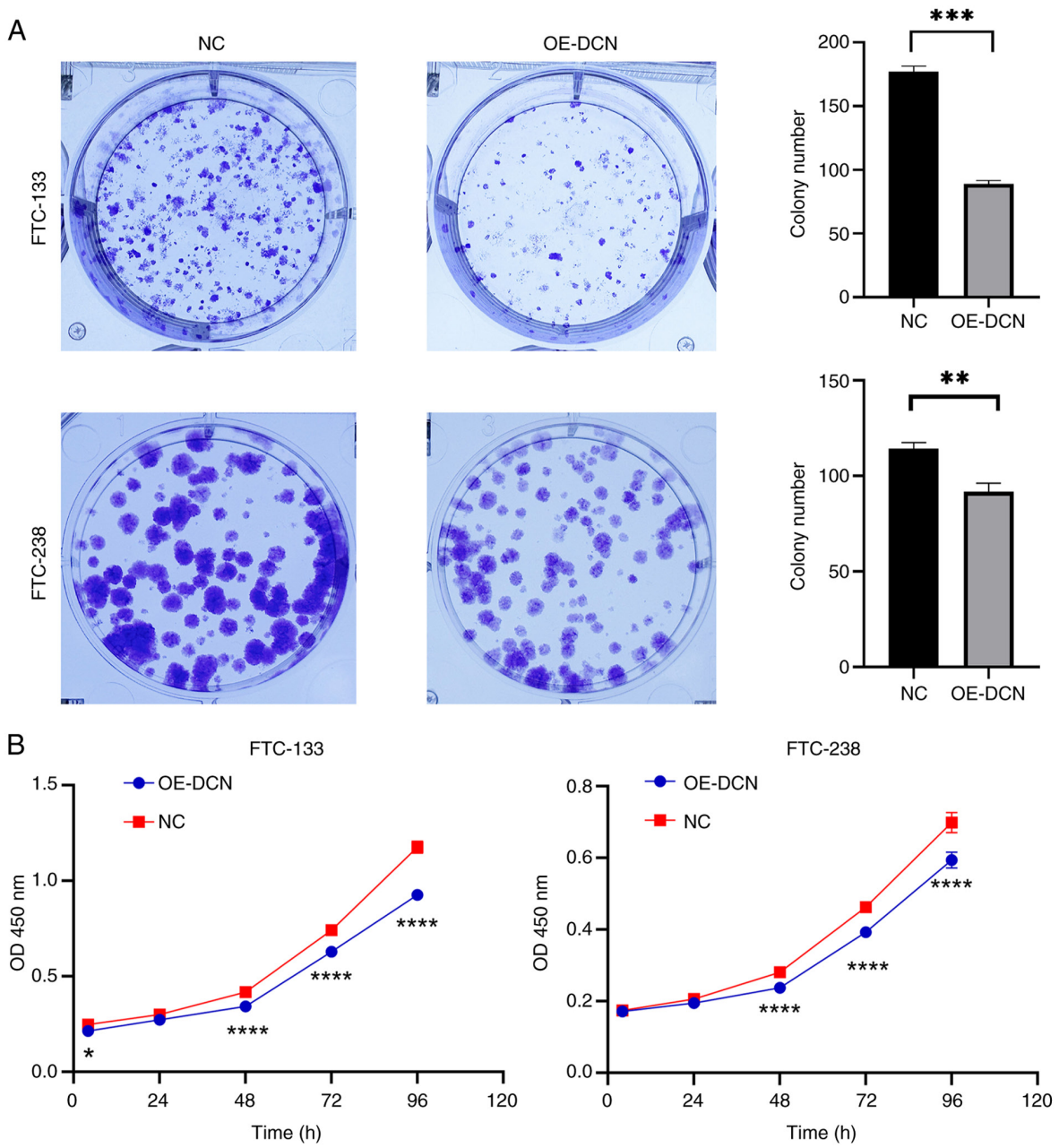

Figure 3. Effects of DCN overexpression on the colony formation and proliferation of FTC-133 and FTC-238 cells. (A) Clonogenic potential assessed through colony formation assays and (B) viability assessed using Cell Counting Kit-8 assays in FTC-133 and FTC-238 cells following DCN overexpression. *P<0.05, **P<0.01, ***P<0.001 and ****P<0.0001 vs. the corresponding NC group. DCN, decorin; OE-DCN, DCN overexpression group; NC, negative control group; OD, optical density.

clonogenic capacity of the OE-DCN groups of FTC-133 and FTC-238 cells was significantly decreased compared with that of the corresponding NC groups (P<0.01; Fig. 3A). In addition, CCK-8 assays demonstrated that cell viability in the OE-DCN groups was significantly lower compared with that in the respective NC groups (P<0.05; Fig. 3B). These findings indicate that DCN overexpression inhibits the proliferation of FTC cells.

DCN overexpression suppresses the invasion and migration of FTC cells. Finally, the effects of DCN overexpression on FTC cell invasion and migration were evaluated. Transwell assay results indicated that DCN overexpression significantly reduced the invasive ability of FTC cells compared with that of the NC group (P<0.05; Fig. 4A). In addition, wound healing assay results demonstrated that DCN overexpression significantly impaired the edge-to-center wound healing of FTC cells relative to that of the respective NC group (P<0.01; Fig. 4B). These findings collectively indicate that DCN overexpression suppresses FTC cell invasion and migration.

Discussion

The increasing prevalence of thyroid carcinoma, particularly DTC, has attracted considerable clinical attention. While early-stage cases often respond favorably to surgical intervention, advanced or recurrent FTC presents substantial therapeutic challenges (16). The American Thyroid Association guidelines emphasize that FTC has a tendency for

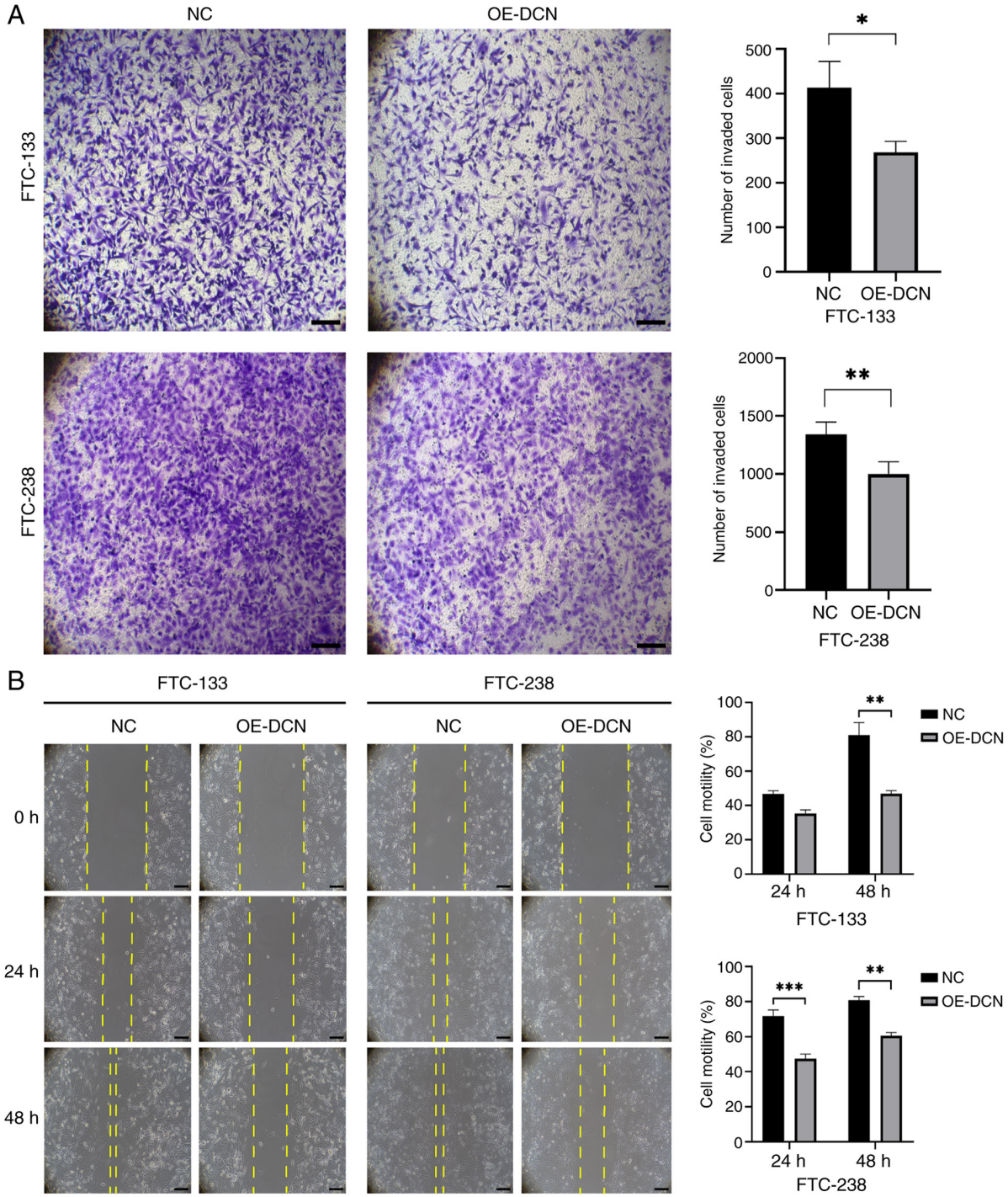

Figure 4. Effects of DCN overexpression on the invasion and migration of FTC-133 and FTC-238 cells. (A) Transwell assay of cell invasion and (B) wound healing assay of cell migration for FTC-133 and FTC-238 cells following DCN overexpression. Scale bars, 100 μm. *P<0.05, **P<0.01 and ***P<0.001 vs. the corresponding NC group. DCN, decorin; OE-DCN, DCN overexpression group; NC, negative control group.

dedifferentiation and resistance to RAI therapy, with 20-30% of patients with distant metastases, such as pulmonary or skeletal metastases, becoming RAI-refractory (RAI-R) (5). Cases with distant metastases demonstrate a marked reduction in 10-year survival rate (<20% for metastatic disease vs. >90% for localized disease) (17), highlighting the importance of understanding FTC pathogenesis and identifying novel therapeutic targets.

DCN, a small leucine-rich PG, has been recognized as a potent tumor suppressor across various malignancies. For example, in inflammatory breast cancer, DCN suppresses invasion and tumor growth by destabilizing E-cadherin and inhibiting EGFR/ERK signaling (7). DCN also inhibits breast cancer metastasis through its anti-lymphangiogenic functions (8). In addition, in hepatocellular carcinoma, DCN deficiency has been associated with increased tumorigenesis via mechanisms involving cell cycle arrest, caspase-3 activation and the suppression of proliferation (9,10). Similarly, studies using colorectal cancer models have demonstrated that the downregulation of DCN expression promotes hepatic

metastasis by dysregulating receptor tyrosine kinases (11,12). Arnaldi *et al* (13) extended these observations to FTC, reporting reduced DCN mRNA levels in follicular thyroid tumors. Furthermore, our previous study corroborated these findings at the histological and cellular levels, revealing significant downregulation of DCN in FTC tissues and cell lines (14). This convergence of evidence indicates that DCN is a molecular regulator of tumor suppression across diverse malignancies, including FTC.

Expanding upon our previous histological and bioinformatics study (14), which identified DCN as a differentially expressed gene in FTC and verified its diminished protein abundance in tumor tissues, the present study aimed to elucidate its functional significance. Two principal advancements were achieved: Firstly, comparative analyses revealed that DCN expression in FTC cell lines was significantly downregulated compared with that in normal thyroid follicular cells, extending tissue-level observations to *in vitro* models. Secondly, lentivirus-mediated DCN overexpression in FTC-133 and FTC-238 cells significantly suppressed their malignant phenotypes, as evidenced by reduced viability and decreased migration and invasion capabilities. These findings establish a direct association between increased DCN expression and suppressed FTC aggressiveness, providing functional validation of the mRNA-level observations reported by Arnaldi *et al* (13).

While the present study offers valuable insights, several limitations require consideration. Firstly, the mechanistic foundations of the antitumor effects of DCN remain unexplored; its downstream signaling pathways merit investigation in future studies. Secondly, the findings are derived only from two FTC cell lines; validation across additional models, such as primary tumor cells or patient-derived xenografts, would enhance the generalizability of the conclusions. Thirdly, the study lacks *in vivo* evidence; animal models are necessary to confirm the therapeutic potential of DCN. Lastly, clinical associations between DCN expression levels and patient outcomes, including survival and RAI resistance, remain unaddressed, necessitating prospective cohort studies.

In conclusion, the present study supplements previous histological and bioinformatics evidence (14) with functional validation, establishing DCN as a critical tumor suppressor in FTC. DCN overexpression was found to inhibit the proliferation, migration and invasion of FTC cells, suggesting that DCN may suppress FTC progression. These findings highlight the potential of DCN as a therapeutic target for RAI-R FTC. Future research should focus on elucidating the underlying mechanisms, including *in vivo* validation of the therapeutic effects of DCN using animal models such as patient-derived xenografts, and clarification of the downstream signaling pathways through which DCN exerts its antitumor activity; the EGFR/ERK and MAPK/PI3K-AKT pathways are suggested as potential candidates. Proteomic profiling and single-cell RNA sequencing could further uncover DCN-regulated molecular networks and cellular heterogeneity in FTC dedifferentiation and RAI resistance. Preclinical validation of DCN-based strategies, along with clinical studies investigating the association of DCN expression with metastatic progression and therapeutic outcomes, will be essential for advancing its translation into targeted therapies for aggressive FTC.

Acknowledgements

Not applicable.

Funding

This study received financial support from the Young Fund Project of the Jiading District Health Commission, Shanghai (grant no. 2021-QN-02), Project of the Science and Technology Commission of Jiading District, Shanghai, China (grant no. JDKW-2022-0016) and General Project of the Shanghai Jiading District Health Commission, China (grant no. 2022-KY-13).

Availability of data and materials

The data generated in the present study may be requested from the corresponding author.

Authors' contributions

QL was responsible for experimental design, data analysis and manuscript preparation. YM and XW were responsible for data acquisition. HG contributed to the experimental design, supervised the execution of experiments and critically reviewed the statistical methodology. TY provided conceptual guidance for the study, interpreted key findings related to clinical relevance and revised the manuscript for intellectual content. RG participated in data interpretation, validated the pathological significance of results and substantially edited the manuscript. HG and RG confirm the authenticity of all the raw data. All authors read and approved the final version of the manuscript.

Ethics approval and consent to participate

Not applicable.

Patient consent for publication

Not applicable.

Competing interests

The authors declare that they have no competing interests.

References

1. Sung H, Ferlay J, Siegel RL, Laversanne M, Soerjomataram I, Jemal A and Bray F: Global cancer statistics 2020: GLOBOCAN estimates of incidence and mortality worldwide for 36 cancers in 185 countries. CA Cancer J Clin 71: 209-249, 2021.
2. Chiapponi C, Hartmann MJM, Schmidt M, Faust M, Schultheis AM, Bruns CJ and Alakus H: Radioiodine refractory follicular thyroid cancer and surgery for cervical relapse. Cancers (Basel) 13: 6230-6240, 2021.
3. Luvhengo TE, Bombil I, Mokhtari A, Moeng MS, Demetriou D, Sanders C and Dlamini Z: Multi-omics and management of follicular carcinoma of the thyroid. Biomedicines 11: 1217, 2023.

4. Vuong HG, Le MK, Hassell L, Kondo T and Kakudo K: The differences in distant metastatic patterns and their corresponding survival between thyroid cancer subtypes. Head Neck 44: 926-932, 2022.
5. Haugen BR, Alexander EK, Bible KC, Doherty GM, Mandel SJ, Nikiforov YE, Pacini F, Randolph GW, Sawka AM, Schlumberger M, *et al*: 2015 American thyroid association management guidelines for adult patients with thyroid nodules and differentiated thyroid cancer: The American thyroid association guidelines task force on thyroid nodules and differentiated thyroid cancer. Thyroid 26: 1-133, 2016.
6. Dong Y, Zhong J and Dong L: The role of decorin in autoimmune and inflammatory diseases. J Immunol Res 2022: 1283383, 2022.
7. Hu X, Villodre ES, Larson R, Rahal OM, Wang X, Gong Y, Song J, Krishnamurthy S, Ueno NT, Tripathy D, *et al*: Decorin-mediated suppression of tumorigenesis, invasion, and metastasis in inflammatory breast cancer. Commun Biol 4: 72, 2021.
8. Mondal DK, Xie C, Pascal GJ, Buraschi S and Iozzo RV: Decorin suppresses tumor lymphangiogenesis: A mechanism to curtail cancer progression. Proc Natl Acad Sci USA 121: e2317760121,2024.
9. Horváth Z, Kovalszky I, Fullár A, Kiss K, Schaff Z, Iozzo RV and Baghy K: Decorin deficiency promotes hepatic carcinogenesis. Matrix Biol 35: 194-205, 2014.
10. Reszegi A, Horváth Z, Fehér H, Wichmann B, Tátrai P, Kovalszky I and Baghy K: Protective role of decorin in primary hepatocellular carcinoma. Front Oncol 10: 645, 2020.
11. Bi X, Pohl NM, Qian Z, Yang GR, Gou Y, Guzman G, Kajdacsy-Balla A, Iozzo RV and Yang W: Decorin-mediated inhibition of colorectal cancer growth and migration is associated with E-cadherin in vitro and in mice. Carcinogenesis 33: 326-330, 2012
12. Reszegi A, Horváth Z, Karászi K, Regős E, Postniková V, Tátrai P, Kiss A, Schaff Z, Kovalszky I and Baghy K: The protective role of decorin in hepatic metastasis of colorectal carcinoma. Biomolecules 10: 1199, 2020.
13. Arnaldi LA, Borra RC, Maciel RM and Cerutti JM: Gene expression profiles reveal that DCN, DIO1, and DIO2 are underexpressed in benign and malignant thyroid tumors. Thyroid 15: 210-221, 2005.
14. Lin Q, Ma Y and Chen P: Identification of potential biomarkers in follicular thyroid carcinoma: Bioinformatics and immunohistochemical analyses. Oncologie 26: 311-322, 2024.
15. Livak KJ and Schmittgen TD: Analysis of relative gene expression data using real-time quantitative PCR and the 2(-delta delta C(T)) method. Methods 25: 402-408, 2001.
16. Phay JE and Ringel MD: Metastatic mechanisms in follicular cell-derived thyroid cancer. Endocr Relat Cancer 20: R307-R319, 2013.
17. Karapanou O, Simeakis G, Vlassopoulou B, Alevizaki M and Saltiki K: Advanced RAI-refractory thyroid cancer: An update on treatment perspectives. Endocr Relat Cancer 29: R57-R66, 2022.